

## Localized Eigenmodes in a Triangular Multicore Hollow Optical Fiber for Space-division Multiplexing in C+L Band

Seongjin Hong and Kyunghwan Oh\*

*Institute of Physics and Applied Physics, Yonsei University, Seoul 03722, Korea*

(Received February 20, 2018 : revised May 31, 2018 : accepted June 4, 2018)

We propose a triangular-multicore hollow optical fiber (TMC-HOF) design for uncoupled mode-division and space-division multiplexing. The TMC-HOF has three triangular cores, and each core has three modes:  $LP_{01}$  and two split  $LP_{11}$  modes. The asymmetric structure of the triangular core can split the  $LP_{11}$  modes. Using the proposed structures, nine independent modes can propagate in a fiber. We use a fully vectorial finite-element method to estimate effective index, chromatic dispersion, differential group delay (DGD), and confinement loss by controlling the parameters of the TMC-HOF structure. We confirm that the proposed TMC-HOF shows flattened chromatic dispersion, low DGD, low confinement loss, low core-to-core crosstalk, and low crosstalk between adjacent modes. The proposed TMC-HOF can provide a common platform for MDM and SDM applications.

*Keywords* : Triangular core optical fiber, Mode-division multiplexing, Space-division multiplexing, Multicore fiber

*OCIS codes* : (060.0060) Fiber optics and optical communications; (060.4510) Optical communication; (060.2330) Fiber optics communications; (230.7370) Waveguides

### I. INTRODUCTION

The amount of data is exploding, in the era of Big Data and its applications [1-4]. It is reported that the transmission system of optical networking along a conventional single-mode fiber (SMF) is approaching its physical limits [5, 6]. To solve this problem, various methods are being investigated to increase the optical transmission capacity [7-9]. First, space-division multiplexing (SDM) with multicore fiber (MCF) is recognized as a straightforward way to address data traffic; it offers a certain solution, to increase data transmission density with high core count [10, 11]. The key challenges for MCF are low loss, and low core-to-core crosstalk [12]. By controlling structural parameters such as index profile and core geometry, a MCF can have low loss, and low core-to-core crosstalk [12]. Second, mode-division multiplexing (MDM) based on few-mode fiber (FMF) also can be a practical solution to increasing data [13, 14]. MDM utilizes individual

orthogonal modes in a FMF as separate carriers. The main feature of MDM is the low mode coupling in the FMF [15]. It has been reported that to suppress crosstalk between two adjacent modes, the effective-index difference  $\Delta n_{eff}$  should be greater than  $\sim 10^{-4}$  [16], which can be realized by controlling the structural parameters and index profile [17].

Recently the authors have introduced an optical fiber with a circular hole at the center surrounded by three triangular cores [18, 19], which is composed of an air-germanosilica core with silica cladding. It shows a significant advantage in the fabrication process compared to previous MCFs, because only one Ge-doped silica tube is needed to make three cores in a fiber. It can be used for both SMD and MDM, because it has orthogonal modes in a core as well as three multicores.

In this study we focus on its asymmetric structure for split  $LP_{11}$  modes, such that applying its unique, asymmetric triangular structure can break the circular symmetry of  $LP$  modes in a fiber and split the degenerate  $LP_{11}$  mode into

\*Corresponding author: [koh@yonsei.ac.kr](mailto:koh@yonsei.ac.kr), ORCID 0000-0003-2544-0216

Color versions of one or more of the figures in this paper are available online.



This is an Open Access article distributed under the terms of the Creative Commons Attribution Non-Commercial License (<http://creativecommons.org/licenses/by-nc/4.0/>) which permits unrestricted non-commercial use, distribution, and reproduction in any medium, provided the original work is properly cited.

two. We further investigate the guiding properties of a TMC-HOF in the C+L bands by controlling its structural parameters. Numerical modal analyses are performed using a fully vectorial finite-element method (FEM) with the perfectly matched layer (PML) boundary condition [20]. This waveguide structure provides three orthogonal modes,  $LP_{01}$  and two split  $LP_{11}$  modes, in each of the cores, and has low core-to-core crosstalk and low crosstalk between adjacent modes in the C and L bands. The three spatially uncoupled modes can propagate in each core of the fiber, which enables MDM optical transmission, and the three cores in our fiber also can realize SDM optical communication with low core-to-core crosswalk. Our proposed waveguide structure supports a total of nine independent, uncoupled optical transmission routes in a single fiber. Therefore, the proposed TMC-HOF can provide a unique platform to enable MDM and SDM simultaneously, allowing multiple-input-multiple output (MIMO) processing in high capacity optical-fiber communication. Therefore, the proposed TMC-HOF can provide a common platform for MDM and SDM optical-fiber communication.

## II. PROPOSED WAVEGUIDE AND STRUCTURAL PARAMETERS

The cross section of the proposed TMC-HOF structure is shown in Fig. 1(a). The cladding material is pure silica, the optical dispersion of which was calculated using the Sellmeier equation for vitreous silica glass. In reference to silica, the triangular core has an index difference  $\Delta n = 0.5\%$ , the optical properties being calculated using the Sellmeier equation for  $GeO_2$ -doped silica glass [21]. The circular air hole is surrounded by three triangular cores. The structure

of the cores is shown in Fig. 1(b).  $R$ , the distance from the center to a vertex of the large triangle, is adjusted to find the optimized structure size for low core-to-core crosstalk, low confinement loss, and  $\Delta n_{eff}$  between adjacent modes for low crosstalk. In the optimized TMC-HOF design, we obtained 3 eigenmodes:  $LP_{01}$ ,  $LP_{11a}$ , and  $LP_{11b}$ , as shown in Fig. 1(d). Figure 1(c) shows a real image of a fabricated TMC-HOF at  $\lambda = 632.8$  nm.

Using vectorial FEM with the PML condition, modal analysis is carried out for our TMF. The magnetic field propagating along the  $z$  direction in the fiber can be expressed as:

$$\vec{H}(x, y, z, t) = \vec{H}(x, y) \exp[i(\omega t - \beta z)] \quad (1)$$

where  $\beta$  is the propagation constant and  $\omega$  is the angular frequency. Eq. (2) shows an eigenvalue equation for the magnetic field in the steady state with a refractive index distribution  $n$ .

$$\nabla \times (n^{-2}(\omega) \times \vec{H}) - k_0^2 \vec{H} = 0 \quad (2)$$

where  $k_0$  is given by  $\omega/c$  and  $c$  is the speed of light. The Sellmeier equation is used to evaluate the wavelength-dependent refractive index for the silica cladding and  $GeO_2$ -doped silica core regions, to account for correct material dispersion. By using FEM, Eq. (2) is solved with triangular meshes to find  $\beta$ . Subsequently the effective mode index  $n_{eff}$  of the guided mode is obtained by taking the real part of  $\beta/k_0$ , while confinement loss is obtained from its imaginary part [22]. In the analysis, boundary conditions for the inner elements were set to satisfy the continuity conditions, and the outer boundary was set to

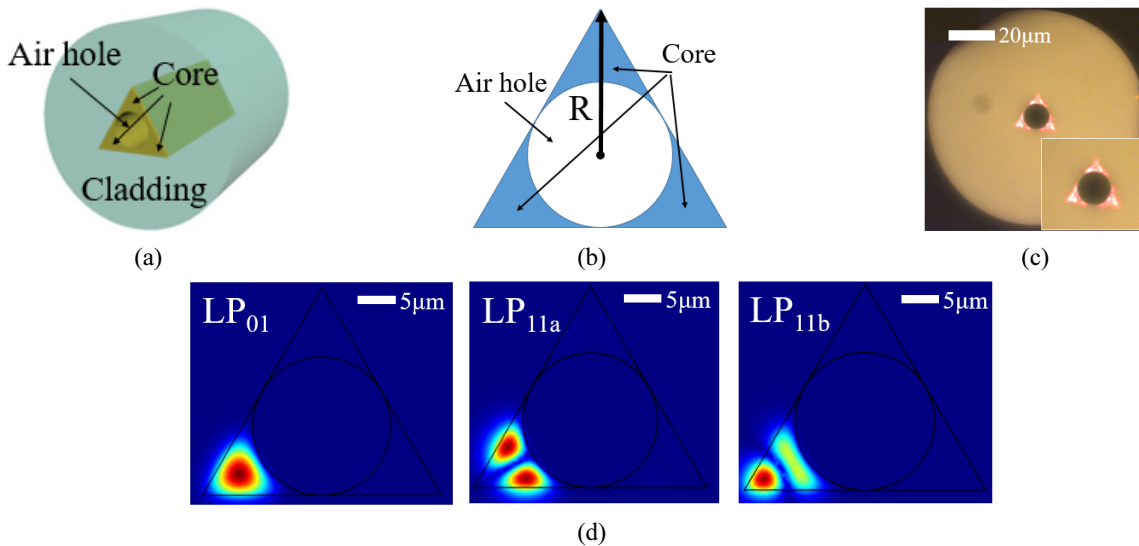


FIG. 1. Schematic diagram of the proposed fiber structure with three triangular core regions: (a) structure of the TMC-HOF, (b) structure of the entire core, (c) cross section of the drawn TMC-HOF with 633-nm visible light propagating, and (d) intensity distributions at  $\lambda = 1550$  nm in a TMC-HOF core, for each of the degenerate eigenmodes  $LP_{01}$ ,  $LP_{11a}$ , and  $LP_{11b}$ .

be continuous with the PML [22].

To confirm that our designed TMC-HOF structure has low crosstalk between cores, we numerically calculate the butt-coupling coefficient between two cores,  $c_{pq}$ , which depends on  $R$  [23]:

$$c_{pq} = \frac{\int (E_p^* \times H_q + E_q \times H_p^*) dA}{\int (E_p^* \times H_p + E_p \times H_p^*) dA} \quad (3)$$

where  $p$  and  $q$  are the indices of two cores among the three. Figure 2 shows that the electric fields of confined modes in the cores depend on  $R$ . The core-to-core crosstalk for  $LP_{01}$  is low, but for  $LP_{11a}$  and  $LP_{11b}$  is

obviously higher, as shown in Fig. 2. The core-to-core crosstalk for  $LP_{11}$  decreases when  $R$  increases, because of the increase in distance between cores. For the  $LP_{11}$  modes we confirm the low core-to-core crosstalk  $c \ll 1$  by calculating  $c_{pq} = 0.0019$  for  $LP_{11a}$  and  $c_{pq} = 0.0011$  for  $LP_{11b}$  at  $\lambda = 1550$  nm, and  $c_{pq} = 0.0052$  for  $LP_{11a}$  and  $c_{pq} = 0.0025$  for  $LP_{11b}$  at  $\lambda = 1625$  nm, when  $R = 33 \mu\text{m}$ . [24, 25]

It is well known that to suppress the crosstalk between adjacent modes,  $\Delta n_{eff}$  should be greater than  $\sim 10^{-4}$  [16]. We numerically calculate  $\Delta n_{eff}$  between  $LP_{11a}$  and  $LP_{11b}$  to confirm that it is higher than  $\sim 10^{-4}$ . The effective refractive index of each mode is plotted as a function of  $R$  in Fig. 3(a), from which we can confirm that the proposed waveguide structure allows three-mode guidance in a core

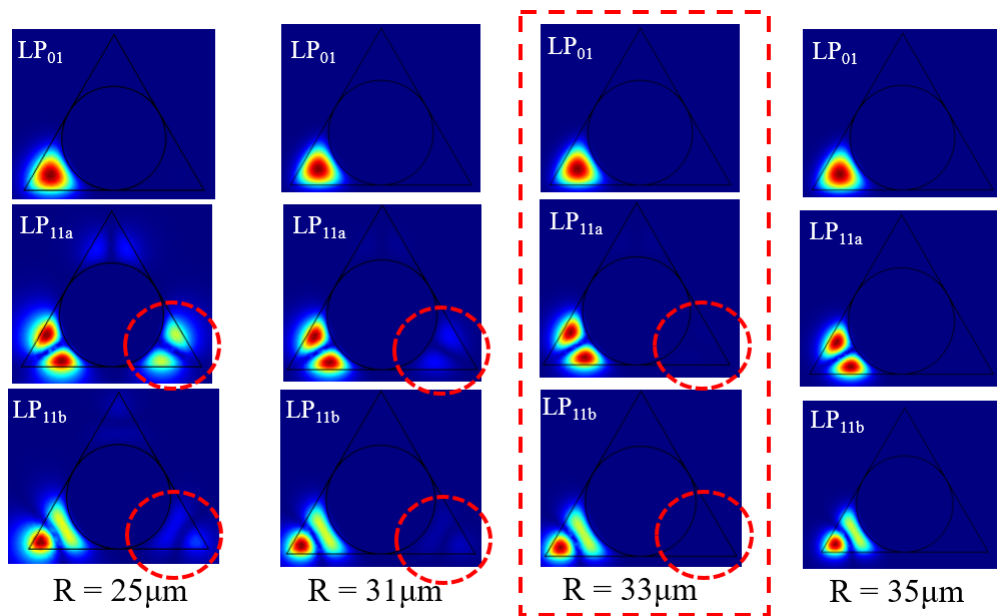


FIG. 2. The intensity distributions in the TMC-HOF for each degenerate mode, depends on  $R$ . It is seen that core-to-core crosstalk disappears when  $R$  is  $33 \mu\text{m}$  or greater.

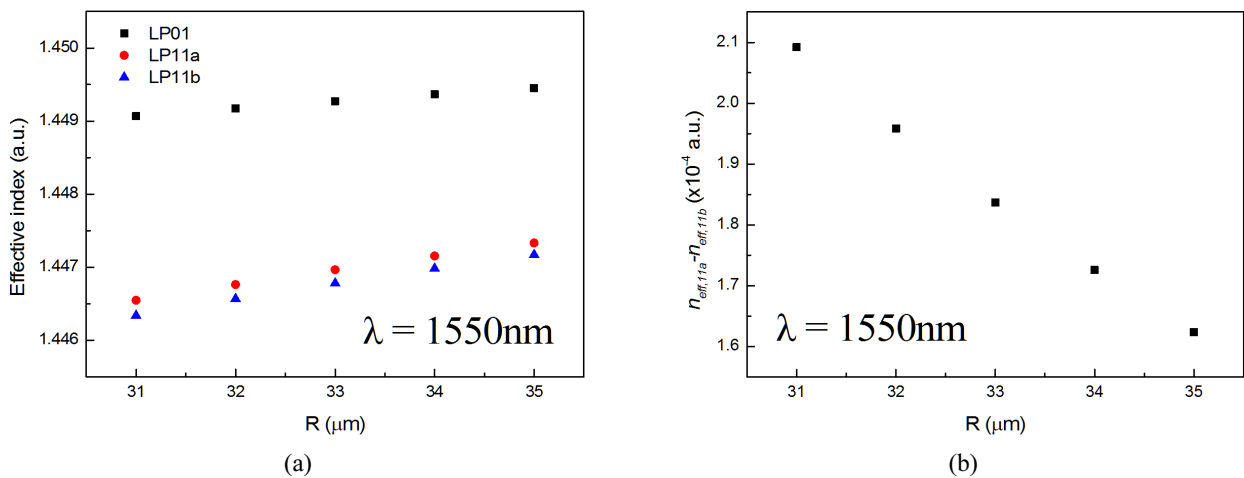


FIG. 3. (a) Variation of effective index of  $LP_{01}$ ,  $LP_{11a}$ , and  $LP_{11b}$  with  $R$ . (b) Effective-index difference between  $LP_{11a}$  and  $LP_{11b}$ , depending on  $R$ .

for MDM. Figure 3(b) shows  $\Delta n_{eff}$  between  $LP_{11a}$  and  $LP_{11b}$ , and we can confirm that the  $LP_{11}$  mode is split into two modes with  $\Delta n_{eff}$  greater than  $10^{-4}$ , suitable for use in MDM. It is possible to fabricate the TMC-HOF of previous reports, and we optimize the structural size as  $R=33 \mu\text{m}$  at  $\Delta n=0.5\%$  for C and L -band communication [26].

### III. MODAL CHARACTERISTICS OF THE TMC-HOF

To confirm that our proposed waveguide structure allows three-mode guidance when  $R=33 \mu\text{m}$  at  $\Delta n=0.5\%$ , we carry out a numerical calculation of the effective indices of modes  $LP_{01}$ ,  $LP_{11a}$ , and  $LP_{11b}$ . Figure 4(a) shows the effective mode index of each as a function of wavelength, in the C and L bands. We also investigate the splitting of the  $LP_{11}$  mode into  $LP_{11a}$  and  $LP_{11b}$ , as shown in Fig. 4(b).

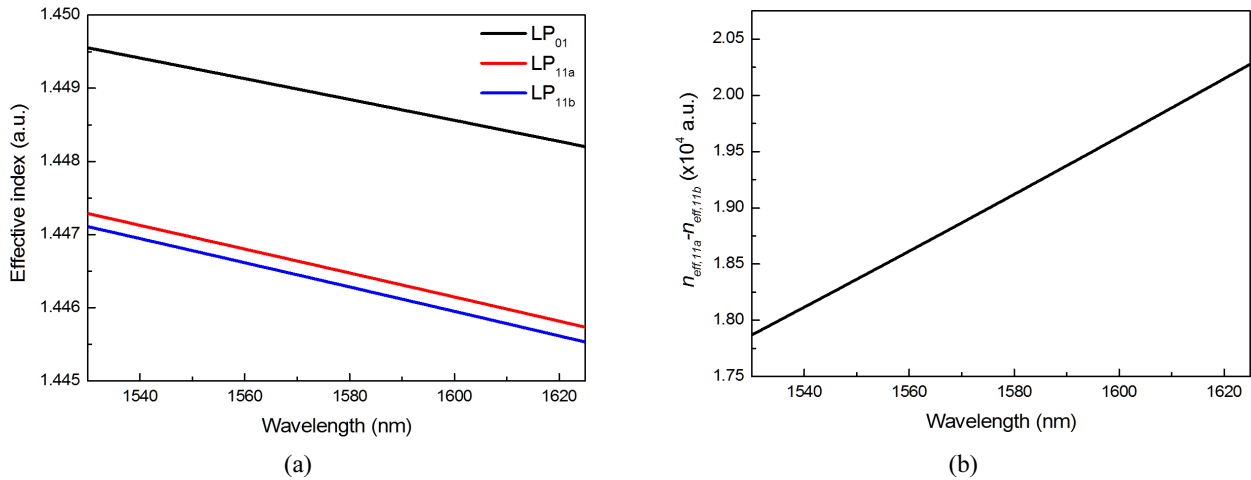


FIG. 4. (a) Variation of effective index of  $LP_{01}$ ,  $LP_{11a}$ , and  $LP_{11b}$  modes in the C and L bands. (b) Effective-index difference between  $LP_{11a}$  and  $LP_{11b}$  modes in the C and L bands.

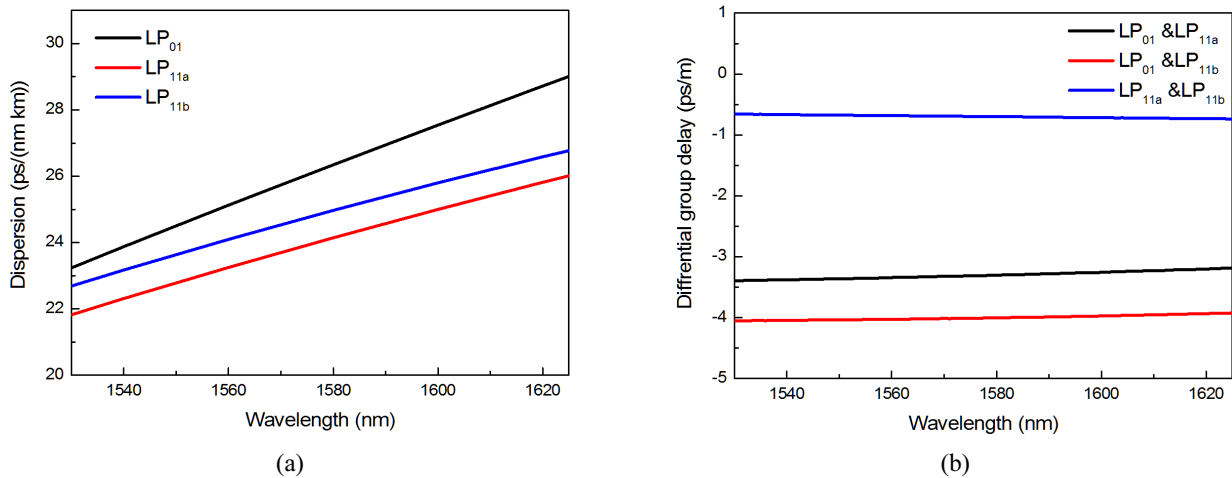


FIG. 5. (a) Chromatic dispersion of  $LP_{01}$ ,  $LP_{11a}$ , and  $LP_{11b}$  modes in the C+L-band spectral range. (b) Differential group delay between pairs among the  $LP_{01}$ ,  $LP_{11a}$ , and  $LP_{11b}$  modes in the C+L-band spectral range.

The  $LP_{11}$  mode is split into the two modes  $LP_{11a}$ , and  $LP_{11b}$ , because of the unique, asymmetric triangular structure.  $\Delta n_{eff}$  between  $LP_{11a}$  and  $LP_{11b}$  is calculated to be greater than  $10^{-4}$  for suppression of mode coupling, and monotonically increases from  $1.78 \times 10^{-4}$  to  $2.02 \times 10^{-4}$ , depending on the wavelength in the C and L bands. This ensures that the three modes are guided well along a core of the proposed TMC-HOF.

The chromatic dispersion of the  $LP_{01}$ ,  $LP_{11a}$ , and  $LP_{11b}$  modes in our TMC-HOF is calculated as a function of wavelength using the real part of  $n_{eff}$  and Eq. (4) [27]:

$$Dispersion = -\frac{\lambda}{c} \left( \frac{\partial^2 n_{eff}}{\partial \lambda^2} \right) \quad (4)$$

The results are summarized in Fig. 5(a). The dispersion of  $LP_{01}$  is found to be between 23 and 29 ps/(km nm),

while the dispersions of LP<sub>11a</sub> and LP<sub>11b</sub> are between 22 and 26 ps/(km nm) over the entire C and L bands. These chromatic dispersion values are flattened, compared to that for a commercial single-mode fiber in the C and L bands [28].

Next, DGD is calculated for each pair of modes. We calculate DGD using Eq. (5) between LP<sub>01</sub> and LP<sub>11a</sub>, between LP<sub>01</sub> and LP<sub>11b</sub>, and between LP<sub>11a</sub> and LP<sub>11b</sub> [29].

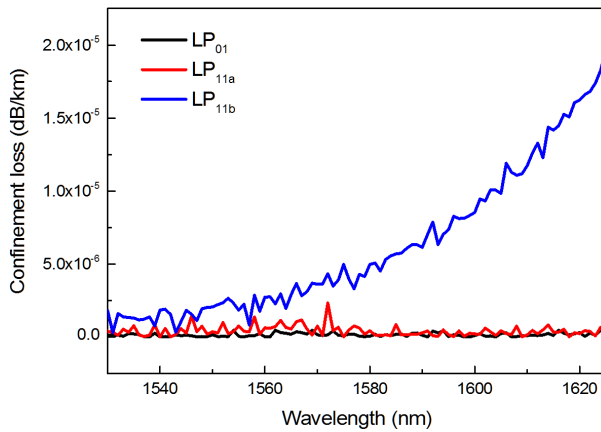
$$DGD = \left( \frac{n_{eff,a} - n_{eff,b}}{c} \right) - \frac{\lambda}{c} \left( \frac{\partial n_{eff,a}}{\partial \lambda} - \frac{\partial n_{eff,b}}{\partial \lambda} \right) \quad (5)$$

where  $n_{eff,a}$  and  $n_{eff,b}$  are the effective indices of each mode respectively, and  $c$  is the speed of light. The results are summarized in Fig. 5(b). DGD for each pair of modes is plotted as a function of wavelength over the entire C and L bands, and the values are seen to be quite comparable to those for prior step-index few-mode fibers [30]. This low DGD is important for simplifying MIMO processing at the receiver [31].

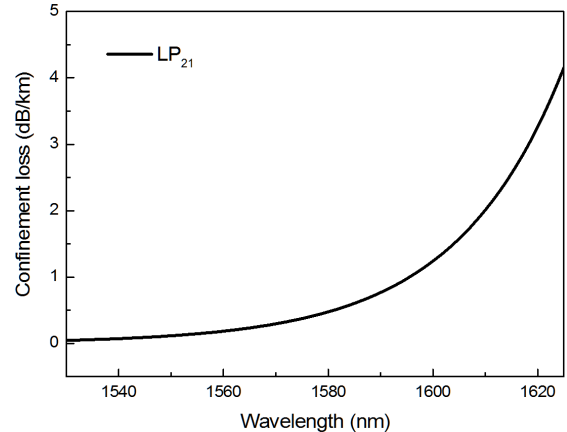
Furthermore, the confinement loss  $\alpha$  (in dB/km) is calculated using fully vectorial FEM analysis with the PML condition from the imaginary part of the propagation constant  $\beta$  [32].

$$\alpha = 20 \log_{10}(e) \cdot \text{Im}(\beta) \quad (6)$$

To properly guide a mode along a fiber, the confinement loss should be less than  $10^{-4}$  dB/km in the spectral range of interest. Figure 6(a) shows that the confinement losses of the LP<sub>01</sub>, LP<sub>11a</sub>, and LP<sub>11b</sub> modes are all less than  $10^{-4}$  dB/km in our wavelength range. We confirm that our proposed TMC-HOF would provide sufficient guidance for all of the modes LP<sub>01</sub>, LP<sub>11a</sub>, and LP<sub>11b</sub>. In contrast, the confinement loss of mode LP<sub>21</sub> is as large as a few dB/km, as shown in Fig. 6(b), which confirms that our TMC-HOF indeed guides only the three modes LP<sub>01</sub>, LP<sub>11a</sub>, and LP<sub>11b</sub>.



(a)



(b)

FIG. 6. Confinement loss of (a) the LP<sub>01</sub>, LP<sub>11a</sub>, and LP<sub>11b</sub> modes, and (b) the LP<sub>21</sub> mode, in the C+L-band spectral range.

Since splicing to conventional SMF is essential to utilize FMF in practical applications, the loss through a SMF-FMF splice must be considered in FMF design. The splice loss is calculated using Eq. (7) [33]:

$$\alpha_{couplingloss} \text{ (dB)} = -20 \log \left[ \frac{2\omega_{SMF}\omega_{TMC-HOF}}{\omega_{SMF}^2 + \omega_{TMC-HOF}^2} \right] \quad (7)$$

where  $\omega_{SMF}$  and  $\omega_{TMC-HOF}$  are the mode-field diameters of the proposed SMF and TMC-HOF respectively. We use  $\omega_{SMF} = 10.2 \mu\text{m}$  [34], while  $\omega_{TMC-HOF}$  is calculated using Eq. (8) [35]:

$$\omega_{TMC-HOF} = \sqrt{\frac{A_{eff}}{\pi}} \quad (8)$$

In the proposed TMC-HOF, the calculated value of splice loss into SMF is 1.456 dB, and could be decreased using an adiabatic mode-conversion process [36].

#### IV. CONCLUSION

We have designed a TMC-HOF for uncoupled MDM and SDM applications. Our proposed TMC-HOF waveguide, based on its unique, asymmetric triangular structure, can split the LP<sub>11</sub> mode into two modes, LP<sub>11a</sub> and LP<sub>11b</sub>. We have successfully reduced the core-to-core crosstalk, and the crosstalk between the LP<sub>11a</sub> and LP<sub>11b</sub> modes. Using a fully vectorial finite-element method, we optimized the structural size of the designed TMC-HOF so that it can guide the three LP modes with  $\Delta n_{eff}$  greater than  $10^{-4}$  in the C and L bands. Our proposed waveguide structure supports a total of nine independent, uncoupled optical transmission routes in a single fiber. Additionally, the proposed TMC-HOF shows flattened chromatic dispersion, low DGD, and low confinement loss, which confirms that

the waveguide can provide a common platform for MDM and SDM applications simultaneously, allowing MIMO processing in high-capacity optical-fiber communication.

### ACKNOWLEDGMENT

This work was supported in part by the ICT R&D Program of MSIP/IITP (2014-3-00524), in part by the Nano Material Technology Development Program through the National Research Foundation of Korea (NRF), funded by the MSIP (NRF-2012M3A7B4049800), and in part by the Basic Science Research Program through the NRF, funded by the Ministry of Science, ICT & Future Planning (No. 2016k1A3A1A09918616).

### REFERENCES

1. L. Schares, B. G. Lee, F. Checoni, R. Budd, A. Rylyakov, N. Dupuis, F. Petrini, C. L. Schow, P. Fuentes, and O. Mattes, "A throughput-optimized optical network for data-intensive computing," *IEEE Micro* **34**, 52-63 (2014).
2. E. Agrell, M. Karlsson, A. Chraplyvy, D. J. Richardson, P. M. Krümmrich, P. Winzer, K. Roberts, J. K. Fischer, S. J. Savory, and B. J. Eggleton, "Roadmap of optical communications," *J. Opt.* **18**, 063002 (2016).
3. M. Gu, X. Li, and Y. Cao, "Optical storage arrays: a perspective for future big data storage," *Light: Sci. Appl.* **3**, e177 (2014).
4. J. Feng and X. Zhao, "Performance analysis of FSO communication systems with photodetector multiplexing," *Curr. Opt. Photon.* **1**, 440-455 (2017).
5. R.-J. Essiambre, G. Kramer, P. J. Winzer, G. J. Foschini, and B. Goebel, "Capacity limits of optical fiber networks," *J. Lightw. Technol.* **28**, 662-701 (2010).
6. R.-J. Essiambre, G. J. Foschini, G. Kramer, and P. J. Winzer, "Capacity limits of information transport in fiber-optic networks," *Phys. Rev. Lett.* **101**, 163901 (2008).
7. C. Xia, N. Bai, I. Ozdur, X. Zhou, and G. Li, "Supermodes for optical transmission," *Opt. Express* **19**, 16653-16664 (2011).
8. F. Yaman, N. Bai, B. Zhu, T. Wang, and G. Li, "Long distance transmission in few-mode fibers," *Opt. Express* **18**, 13250-13257 (2010).
9. T. Hayashi, T. Taru, O. Shimakawa, T. Sasaki, and E. Sasaoka, "Design and fabrication of ultra-low crosstalk and low-loss multi-core fiber," *Opt. Express* **19**, 16576-16592 (2011).
10. D. M. Marom, and M. Blau, "Switching solutions for WDM-SDM optical networks," *IEEE Commun. Mag.* **53**, 60-68 (2015).
11. B. Zhu, T. Taunay, M. Yan, J. Fini, M. Fishteyn, E. Monberg, and F. Dimarcello, "Seven-core multicore fiber transmissions for passive optical network," *Opt. Express* **18**, 11117-11122 (2010).
12. A. Zioliowicz, M. Szymanski, L. Szostkiewicz, T. Tenderenda, M. Napierala, M. Murawski, Z. Holdynski, L. Ostrowski, P. Mergo, and K. Poturaj, "Hole-assisted multicore optical fiber for next generation telecom transmission systems," *Appl. Phys. Lett.* **105**, 081106 (2014).
13. N. Hanzawa, K. Saitoh, T. Sakamoto, T. Matsui, S. Tomita, and M. Koshiba, "Demonstration of mode-division multiplexing transmission over 10 km two-mode fiber with mode coupler," in *Proc. Optical Fiber Communication Conference* (Optical Society of America 2011), p. OWA4.
14. P. Sillard, M. Bigot-Astruc, and D. Molin, "Few-mode fibers for mode-division-multiplexed systems," *J. Lightw. Technol.* **32**, 2824-2829 (2014).
15. P. Sillard, M. Astruc, D. Boivin, H. Maerten, and L. Provost, "Few-mode fiber for uncoupled mode-division multiplexing transmissions," in *Proc. European Conference and Exposition on Optical Communications* (Optical Society of America 2011), p. Tu. 5. LeCervin. 7.
16. N. Riesen, J. D. Love, and J. W. Arkwright, "Few-mode elliptical-core fiber data transmission," *IEEE Photon. Technol. Lett.* **24**, 344 (2012).
17. M. Kasahara, K. Saitoh, T. Sakamoto, N. Hanzawa, T. Matsui, K. Tsujikawa, and F. Yamamoto, "Design of three-spatial-mode ring-core fiber," *J. Lightw. Technol.* **32**, 1337-1343 (2014).
18. W. Ha, S. Lee, J. Kim, Y. Jeong, K. Oh, J. Kobelke, K. Schuster, S. Unger, A. Schwuchow, and J. K. Kim, "A micro-structured aperture made of a hollow triangular-core fiber for novel beam shaping," *Opt. Express* **18**, 20918-20925 (2010).
19. S. Lee, W. Ha, J. Kobelke, K. Schuster, S. Unger, and K. Oh, "Multicorelike guidance in a triangular-core hollow optical fiber and spectral evolution of its eigenmode degeneracy," *Opt. Lett.* **37**, 4759-4761 (2012).
20. Y. S. Lee, C. G. Lee, Y. Jung, M.-K. Oh, and S. Kim, "Highly birefringent and dispersion compensating photonic crystal fiber based on double line defect core," *J. Opt. Soc. Korea* **20**, 567-574 (2016).
21. B. Brixner, "Refractive-index interpolation for fused silica," *J. Opt. Soc. Am.* **57**, 674-676 (1967).
22. M. Park, H. E. Arabi, S. Lee, and K. Oh, "Independent control of birefringence and chromatic dispersion in a photonic crystal fiber using two hollow ring defects," *Opt. Commun.* **284**, 4914-4919 (2011).
23. K. Okamoto, *Fundamentals of optical waveguides* (Academic press, 2010).
24. E. Marcatili, "Improved coupled-mode equations for dielectric guides," *IEEE J. Quantum Electron.* **22**, 988-993 (1986).
25. A. Hardy and W. Streifer, "Coupled mode theory of parallel waveguides," *J. Lightw. Technol.* **3**, 1135-1146 (1985).
26. O. Bands, B. Laurent, and G. Draka, "From O to L: The future of optical-wavelength bands," *Broadband Properties*, 83-85 (2008).
27. K. Oh and U.-C. Paek, *Silica optical fiber technology for devices and components: design, fabrication, and international standards* (John Wiley & Sons, 2012).
28. M. R. Hasan, M. I. Hasan, and M. S. Anower, "Tellurite glass defect-core spiral photonic crystal fiber with low loss and large negative flattened dispersion over S+C+L+U wavelength bands," *Appl. Opt.* **54**, 9456-9461 (2015).
29. L. Grüner-Nielsen, Y. Sun, J. W. Nicholson, D. Jakobsen, K. G. Jespersen, R. Lingle Jr, and B. Pálsdóttir, "Few mode

- transmission fiber with low DGD, low mode coupling, and low loss," *J. Lightw. Technol.* **30**, 3693-3698 (2012).
30. M. Kasahara, K. Saitoh, T. Sakamoto, N. Hanzawa, T. Matsui, K. Tsujikawa, and F. Yamamoto, "Design of three-spatial-mode ring-core fiber," *J. Lightw. Technol.* **32**, 1337-1343 (2014).
  31. F. Ferreira, D. Fonseca, and H. Silva, "Design of few-mode fibers with arbitrary and flattened differential mode delay," *IEEE Photon. Technol. Lett.* **25**, 438-441 (2013).
  32. Y. S. Lee, C. G. Lee, and S. Kim, "Dispersion compensating photonic crystal fiber using double-hole assisted core for high and uniform birefringence," *Optik* **147**, 334-342 (2017).
  33. S. M. A. Razzak and Y. Namihira, "Tailoring dispersion and confinement losses of photonic crystal fibers using hybrid cladding," *J. Lightw. Technol.* **26**, 1909-1914 (2008).
  34. W. H. Reeves, J. C. Knight, and P. S. J. Russell, "Demonstration of ultra-flattened dispersion in photonic crystal fibers," *Electron. Lett.* **38**, 546-547 (2002).
  35. M. Ye, Y. Yang, W. Duan, and M. Yang, "Measure and redress of mode field diameter of polarization maintaining photonic crystal fibers," in *Proc. 8th IEEE International Symposium on Instrumentation and Control Technology (ISICT)*, 101-104 (2012).
  36. S. Choi, K. Oh, W. Shin, and U. C. Ryu, "Low loss mode converter based on adiabatically tapered hollow optical fibre," *Electron. Lett.* **37**, 823-825 (2001).